Oil & Gas Science and Technology – Rev. IFP, Vol. 61 (2006), No. 6, pp. 743-749

DOI: 10.2516/ogst:2006012

Dossier

Deformation of Solid Polymers
Déformation des polymères solides

Non Linear Strain Rate Dependency and Unloading Behavior of Semi-Crystalline Polymers

K. Hizoum[1], Y. Rémond[1], N. Bahlouli[1], V. Oshmyan[2†], S. Patlazhan[2] and S. Ahzi[1]

1 Institut de Mécanique des Fluides et des Solides, Université Louis Pasteur, 2, rue Boussingault, 67000 Strasbourg - France
2 Semenov Institute of Chemical Physics, Russian Academy of Sciences, 4, Kosygin Street, Moscow, 119991 - Russia
e-mail: hizoum@imfs.u-strasbg.fr - remond@imfs.u-strasbg.fr - bahlouli@imfs.u-strasbg.fr - sapat@polymer.chph.ras.ru - ahzi@imfs.u-strasbg.fr

Résumé — Modélisation des non-linéarités en vitesse de déformation et du comportement en déchargement des polymères semi-cristallins — Les lois viscoélastiques classiques ne permettent pas de décrire complètement les comportements caractéristiques des polymères semi-cristallins, comme ceux observés lors de sauts de vitesses ou en déchargement. Nous présentons dans cet article certaines particularités du comportement mécanique pour un polyéthylène ou un polypropylène en petites déformations. Un modèle physique incluant une évolution de la microstructure est présenté et comparé aux observations expérimentales. Ce modèle permet une forte amélioration des simulations des comportements mécaniques en chargement et déchargement pour une large classe de polymères semi-cristallins.

Abstract — Non Linear Strain Rate Dependency and Unloading Behavior of Semi-Crystalline Polymers — *The classical viscoelastic constitutive equations do not simulate correctly the mechanical behavior of semi crystalline polymers, particularly in the case of the strain rate jumping or unloading to zero stress after tensile testing. The main experimental observations of mechanical response of polyethylene and polypropylene at small strains are reviewed. A physical model, which account for the deformation-induced evolution of the material structure, is developed and compared to the experimental observations. It is concluded that this model is the most adequate approach for the simulation of the mechanical behavior and the structure development of semi-crystalline polymers under loading and unloading.*

INTRODUCTION

An abnormal viscoelastic behavior during unloading was observed for a broad class of semi-crystalline polymers (polyethylene, polypropylene, etc.) even at low strains. Many authors were trying to improve modeling of this phenomenon by including:

– different microscopic and macroscopic aspects of structural evolution (Drozdov and Christiansen, 2003; Ahzi *et al*., 2003; Oshmyan *et al*., 2004, 2005, 2006), particularly, crystalline morphology and chain conformations were taken into account for polyethylene (Popelar *et al*., 1990; Hobeika *et al*., 2000; and Sirotkin *et al*., 2001);
– phenomenological viscoelastic or viscoplastic modeling (Yao and Krempl, 1985; Kichenin *et al*., 1996; Chaboche, 1997; Chambaudet *et al*., 1998; Ho and Krempl, 2000; Stehly and Rémond, 2002; Krempl and Ho, 2002; Krempl and Khan, 2003; André *et al*., 2003; Colak, 2004; Rémond, 2005).

The crystalline morphology of polyethylene is highly influenced by the stress over threshold, inducing separation, rotation and torque of the lamellae, the slipping of lamella units, their reorientation inside spherulites, etc. Thus, mechanical behavior of polyethylene under high strains is influenced by the micro structural evolution. Nevertheless, the viscoelastic behavior during both loading and unloading is poorly described especially in a large range of strain rates.

1 PHENOMENOLOGICAL APPROACHES

Consider different approaches in simulation of tensile loading-unloading behavior of semi-crystalline polymers at different strain rates. Figures 1 and 2 show some peculiarities of mechanical response of HDPE and PP under the strain rate jump indicating the strong dependence upon the strain rate. Different approaches were employed to simulate this kind of reaction. For the most part they were based on phenomenological consideration. Particularly, the dynamic behavior of the polymer systems obeys the following equation $\dot{\sigma} = \alpha(\varepsilon.\sigma)\dot{\varepsilon} + \beta(\varepsilon.\sigma)$. For the simple Zener-like models the material functions α and β are taken constants: $\alpha = E_1E_2/\eta$ and $\beta = -(E_1+E_2)\ \sigma/\eta$, where E_1, E_2 and η represent elastic moduli and viscosity of two springs and dashpot respectively. More complicated expressions for α and β had been used to obtain a better simulation of the strain rate jumps (Rémond, 2005). Unfortunately, these approaches do not fit properly the unloading data. Particularly, even if the strain rate jump is simulated accurately, the zero-stress residual strain is overestimated (see *Fig. 3a*). However, if some specific parameters permit obtaining a satisfactory results in simulation complete loading-unloading diagrams under the fixed strain rate, the change of the strain rate will lead to modification of these parameters thus confirming that they are not intrinsic ones (see *Fig. 3b*). Additional three-dimensional approaches were developed using a viscoplastic formulation that takes into account the stress threshold permitting simulation the three-axial viscoelastic behavior (Chaboche, 1997). This allows improving simulation of the unloading by introduction of additional dissipation potential adjusting effect of structure recovering. However this additional potential is not justified by any physical arguments (see *Fig. 4*).

On the other hand, the VBO model corresponding to the viscoplasticity theory based on overstress (Yao and Krempl, 1985) is a known state variable model considering inelastic deformation behavior as a rate dependent. Recently Colak (2004)

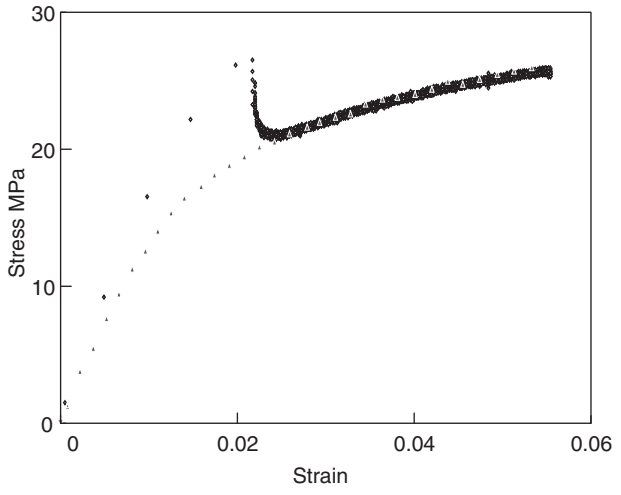

Figure 1

Polyethylene strain rate jump between $\dot{\varepsilon} = 0.1$ and $\dot{\varepsilon} = 0.01$.

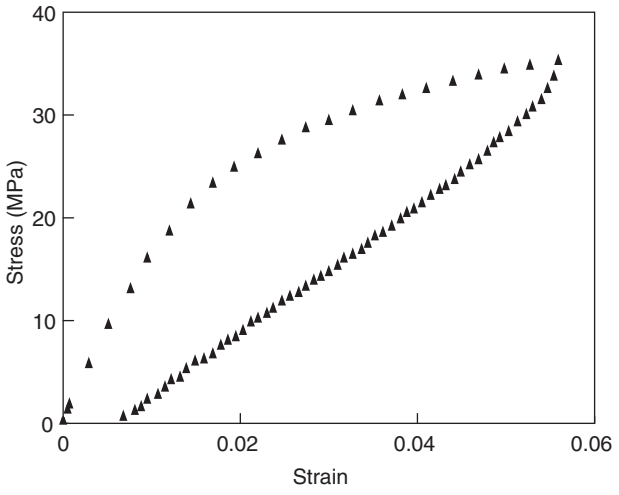

Figure 2

Viscoelastic behaviour of PP Loading rate $\dot{\varepsilon} = 0.05$, unloading rate $\dot{\varepsilon} = 0.02$.

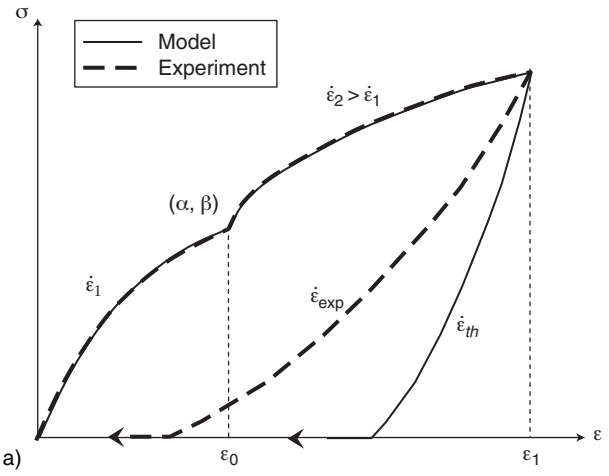

Figure 3a

Constitutive modelling with different loading strain rates.

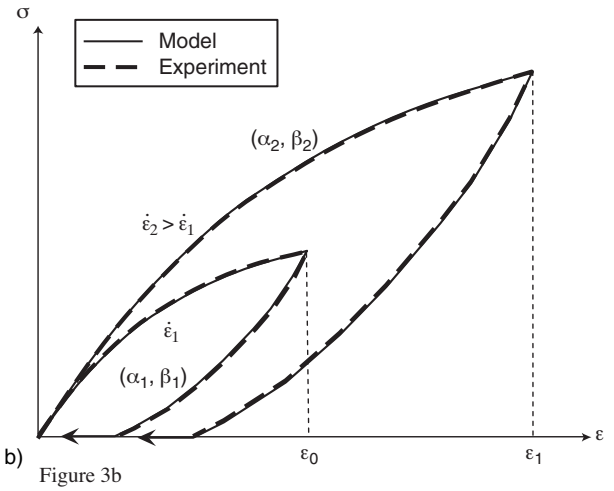

Figure 3b

Constitutive modelling with different strain rates.

has applied this model for simulation of mechanical behavior of polymeric materials under various loading conditions. Descriptions of the creep, the strain recovering and the strain rate jump were got successfully. However, the strain rate dependence at the unloading stage of deformation cannot be modeled precisely.

Concluding this part, constitutive equations based on generalized rheological approaches describe fairly well the load behavior followed by the strain rate jumps. The models developed in the framework of the local state approach can also provide acceptable results in simulation of structures behavior. Nevertheless these phenomenological approaches do not include any link between mechanical behavior and material microstructure. As a result, the model parameters obtained for the loadings parts of the stress-strain diagrams lead often to the underestimation of unloading stresses. The introduction of the complementary potential improving this feature is not physically grounded.

2 EXPERIMENTAL TESTS

Uniaxial tensile tests were performed on a testing machine *Deltalab* DN30 equipped with electro-mechanical sensors for the control of longitudinal strains in the active zone of samples. The samples were produced by injection molding. They were stretched with constant strain rate $\dot{\varepsilon}$ up to different maximum strains $\bar{\varepsilon}$ preceding the unloading:

– $\dot{\varepsilon}=8.3\times10^{-3}S^{-1}$ and $\bar{\varepsilon}$= 0.032, 0.053, 0.072, 0.094 and 0.106 for PP, and

– $\dot{\varepsilon}=5.7\times10^{-4}S^{-1}$ and $\bar{\varepsilon}$= 0.031, 0.061 and 0.09 for LDPE.

Then the samples unloaded with the same strain rate up to zero stress. The strain ranges were taken below the yield stresses corresponding to ε_y=0.13 for PP and ε_y=0.12 for LDPE (Drozdov *et al*., 2003b).

3 MODELING

In this paper we develop the new approach (Oshmyan *et al*., 2004, 2005) which is capable to obtain reasonable simulations of the unloading part of deformation diagrams by accounting for the strain-induced evolution of material structure. Results of this modeling were compared with experiments carried out with low-density polyethylene (LDPE) and polypropylene (PP) at room temperature and the low strain rate. Within this model the stress-induced partial orientation of crystallites was considered effectively by taking into account the strain hardening. This is expressed in increasing of crystallite elastic modulus followed by decreasing of plastic ability (see *Equations 1, 2*). An internal variable responsible for the structural reorganization is included as well. It

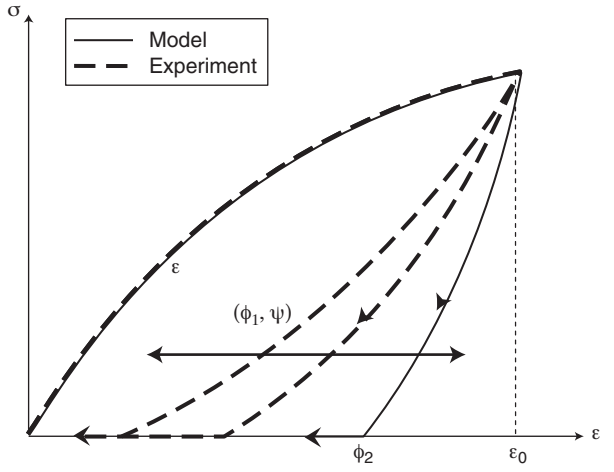

Figure 4

Constitutive modelling with different strain rates.

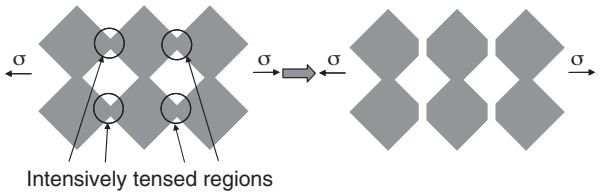

Figure 5

Analogical description of the microstructure.

takes into account sensitivity of structural organization to a current deformation, justified by a local fusion of highly stressed local crystalline zones.

The description of a non linear version of our model is briefly presented here for the case of small-strain behavior. The two-phase material comprised crystalline, (cr), and amorphous, (am), components is considered. The hard phase is represented as an association in series of two elements (viscosity and stiffness) leading to $\varepsilon^{(cr)}=\varepsilon_e^{(cr)}+\varepsilon_p^{(cr)}$ in a limit of small deformations.

The rate of the change of structural parameters is proportional to the applied stress:

$$\frac{\dot{E}^{(cr)}}{E^{(cr)}} = k_E\sigma^{(cr)} \tag{1}$$

$$\frac{\dot{\chi}^{(cr)}}{\chi^{(cr)}} = -k_\chi\sigma^{(cr)} \tag{2}$$

The linear viscoelastic relations between the strain and stress is given by:

$$\sigma^{(cr)}=E^{(cr)}\varepsilon_e^{(cr)} \text{ and } \dot{\varepsilon}_p^{(cr)}=\chi^{(cr)}\sigma^{(cr)} \tag{3}$$

are accepted for the crystalline phase. The amorphous phase is treated as a soft elastic media, $\sigma^{(am)}=E^{(am)}\varepsilon^{(am)}$. Note that plastic ability of the hard phase $\chi^{(cr)}$ corresponds to its inverse viscosity.

Transformation of crystalline to amorphous state of the tensed crystalline regions and, hence, evolution of the crystalline fraction, c, is the most important line of the modeling. The rate of evolution of structural parameter c is also assumed to be proportional to the stress applied:

$$\frac{\dot{c}^{(cr)}}{c^{(cr)}} = -k_c\sigma^{(cr)} \tag{4}$$

A loss of connectivity of the crystalline phase under deformation under the loading (see *Fig. 5*) is considered as a main mechanism of the material softening at unloading. The new portion of the amorphous phase formed by partial transformation of crystals is placed in series with the remaining crystalline phase component at 1D modeling *(Fig. 6)*. Serial connection of structural elements *(Fig. 6)* leads to an additive law for strains:

$$\varepsilon = m\varepsilon^{(cr)} + (1-c)\varepsilon^{(am)} = c\left(\varepsilon_e^{(cr)} + \varepsilon_e^{(am)}\right) + (1-c)\varepsilon^{(am)} \tag{5}$$

and equality of stresses:

$$\sigma = \sigma^{(cr)} = E^{(cr)}\varepsilon_e^{(cr)} = \sigma^{(am)} = E^{(am)}\varepsilon^{(am)} \tag{6}$$

On the other hand, relations:

$$\varepsilon^{(am)} = \frac{E^{(cr)}}{E^{(am)}}\varepsilon_e^{(cr)} \text{and } \varepsilon = c\left(\varepsilon_e^{(cr)} + \varepsilon_p^{(cr)}\right) + \tag{7}$$

$$+(1-c)\frac{E^{(cr)}}{E^{(am)}}\varepsilon_e^{(cr)}$$

lead to the expression for plastic deformation of the crystalline component:

$$\varepsilon_p^{(cr)} = \frac{1}{c}\varepsilon - \left(1 + \frac{1-c}{c}\frac{E^{(cr)}}{E^{(am)}}\right)\varepsilon_e^{(cr)} \tag{8}$$

Combining Equations (1)-(8), we obtain the following system:

$$\begin{cases} \dot{\varepsilon}_e^{(cr)} = \left[\dot{\varepsilon}E^{(am)} + \dfrac{\dot{c}}{c}\left(E^{(cr)}\varepsilon_e^{(cr)} - E^{(am)}\varepsilon\right) - \right. \\ \qquad - \dot{E}^{(cr)}(1-c)\varepsilon_e^{(cr)} - \chi^{(cr)}E^{(cr)}E^{(am)}c\varepsilon_e^{(cr)}\left.\right] / \\ \qquad / \left[(1-c)E^{(cr)} + cE^{(am)}\right] \\ \dot{E}^{(cr)} = k_E E^{(cr)}\varepsilon_e^{(cr)} \\ \dot{\chi}^{(cr)} = -k_\chi E^{(cr)}\varepsilon_e^{(cr)} \\ \dot{c} = -k_c c E^{(cr)}\varepsilon_e^{(cr)} \\ \sigma = \sigma^{(cr)} = E^{(cr)}\varepsilon_e^{(cr)} \end{cases} \tag{9}$$

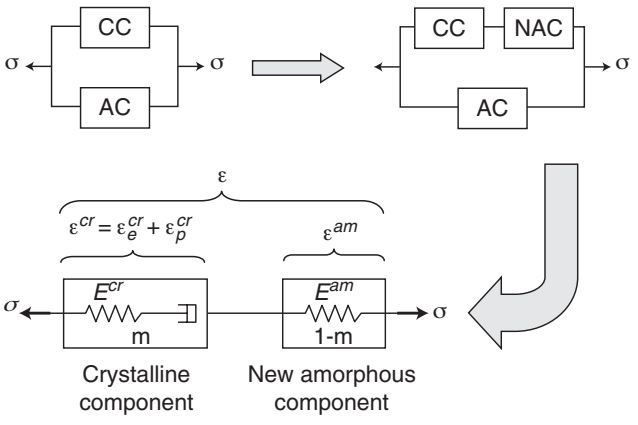

Figure 6

Analogical description of the final model.

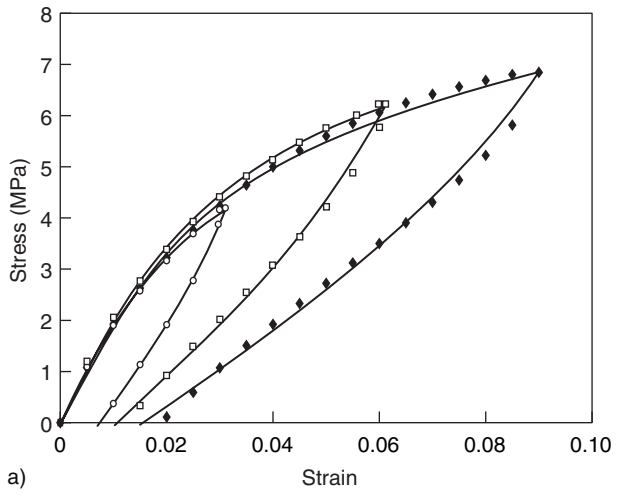

Figure 7a
Loading and unloading OPR modelling for LDPE.

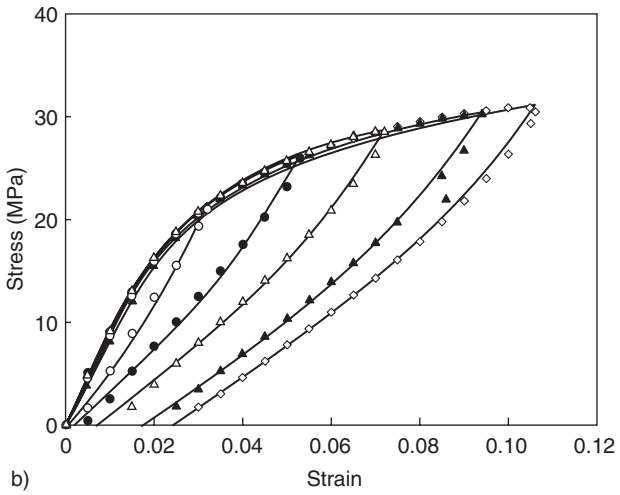

Figure 7b
Loading and unloading OPR modelling for PP.

with the initial conditions:

$$\begin{cases} \varepsilon_e^{(cr)}\big|_{t=0} = 0 \\ E^{(cr)}\big|_{t=0} = E_0^{(cr)} \\ \chi^{(cr)}\big|_{t=0} = \chi_0^{(cr)} \\ c\big|_{t=0} = c_0 \end{cases} \tag{10}$$

These equations were applied to simulate experimental stress-strain diagrams measured for LDPE and PP.

Each loading-unloading curve has been optimized separately (see *Figs. 7a* and *7b*). The optimisation algorithm used is based on the generalized method of least squares. The experimental data $\left(\varepsilon_j^{(\exp)}, \sigma_j^{(\exp)}\right)$, represent $n^{(\exp)}$ experimental points ($j=1..n^{(\exp)}$). Theoretical stresses, $\sigma_j^{(th)}=\sigma^{(th)}\left(p_1, ..., p_n, \varepsilon_j^{(\exp)}\right)$, are calculated by means the given model with the following adjustable parameters: $p_1=E_0^{(cr)}$, $p_2=E^{(am)}$, $p_3=\chi_0^{(cr)}$, $p_4=k_E$, $p_5=k_\chi$, $p_6=c_0$ and $p_7=k_c$. These parameters are derived by minimisation of the function:

$$U\left(p_1,...,p_n\right) = \sum_j \left[\sigma_j^{(th)}\left(p_1,...,p_n,\varepsilon_j^{(\exp)}\right) - \sigma_j^{(ex)}\right]^2 \tag{11}$$

To do so, the following iteration procedure is used. The initial set of parameters $p_i^{(0)}$ is selected near the probable minimum. The iteration steps, $p_i^{(s)} \to p_i^{(s+1)}$, are carried out from the equations:

$$\sum_k \frac{\partial^2 U\left(p_1^{(s)}, p_2^{(s)}, ..., p_n^{(s)}\right)}{\partial p_i \partial p_k} p_k^{(s+1)} = \sum_k \frac{\partial^2 U\left(p_1^{(s)}, p_2^{(s)}, ..., p_n^{(s)}\right)}{\partial p_i \partial p_k} p_k^{(s)} - \frac{\partial U\left(p_1^{(s)}, p_2^{(s)}, ..., p_n^{(s)}\right)}{\partial p_i} \tag{12}$$

followed from the minimum condition $\frac{\partial \tilde{U}\left(p_1, p_2, ..., p_n\right)}{\partial p_i} = 0$.

The approximation function $\tilde{U}(p_1, p_2, ..., p_n)$ is taken as a second-order expansion of $U(p_1, p_2, ..., p_n)$ in the Taylor series:

$$\begin{aligned} &U\left(p_1,p_2,...,p_n\right) \approx \tilde{U}\left(p_1,p_2,...,p_n\right) = \\ &= U\left(p_1^{(s)},p_2^{(s)},...,p_n^{(s)}\right) + \sum_k \frac{\partial U\left(p_1^{(s)},p_2^{(s)},...,p_n^{(s)}\right)}{\partial \boldsymbol{p}_k}\left(p_k - p_k^{(s)}\right) + \\ &+ \frac{1}{2}\sum_{k,l} \frac{\partial^2 U\left(p_1^{(s)},p_2^{(s)},...,p_n^{(s)}\right)}{\partial p_k \partial p_l}\left(p_k - p_k^{(s)}\right)\left(p_l - p_l^{(s)}\right) \end{aligned} \tag{13}$$

The derivatives of U in Equation (11) are calculated numerically on the basis of algorithm developed by Oshmyan *et al.* (2004). This gives a way to obtain parameters $p_i^{(s+1)}$ corresponding to the next step of the iteration procedure and thus approach to their optimal values corresponding to material characteristics of the studied polymers.

The resulted stress-strain curves along with evolution of relative crystallinity are presented in Figures 7a, 7b, and 8. They show that specific features of uniaxial compression deformations of semi-crystalline polymers can be properly described in a framework of the discussed model, accounting evolution of crystalline structure.

In order to assess limits of this approach, our model was applied to simulate two loading-unloading cycles of high-density polyethylene (HDPE). The samples of this polymer were loaded to 5% strain at room temperature and then unloaded to the zero stress. After that they were immediately reloaded to 5% relative to the residual strain and unloaded again. During this test, the strain rate was kept at $\dot{\varepsilon}=1\times10^{-3}s^{-1}$. Figure 9 shows that the predicted results are

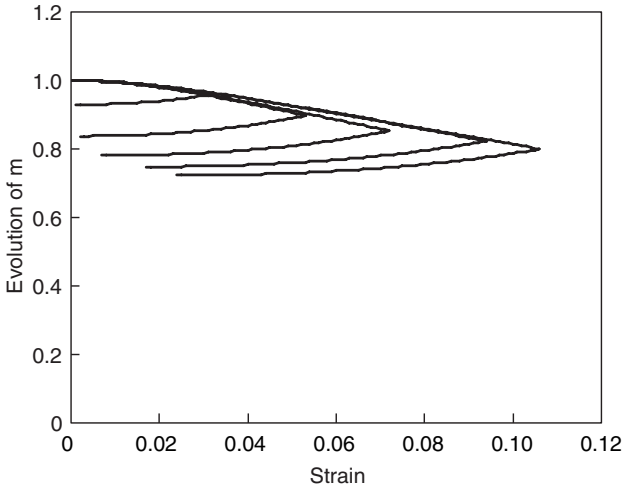

Figure 8

Evolution of the microstructure at low strains.

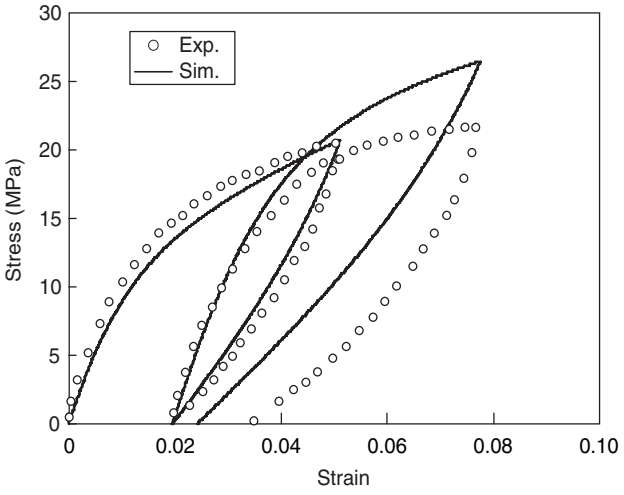

Figure 9

Comparison loading and unloading (two cycles) developed by OPR for HDPE.

in a good agreement just with a first loading-unloading cycle while it is not the case with the second one. The origin of this discrepancy is in the linear dependence of plastic flow rate on the applied stress (see *Equation 3*). This linear approach is shown (Oshmyan *et al*., 2005) to be justified just at small stresses or accompanying deformations. The more general behavior of the plastic strain rate obeys to Eyring law:

$$\dot{\varepsilon}_p^{(cr)} = \dot{\varepsilon}_{p0}^{(cr)} \exp\left(-\frac{U^{(cr)}}{kT}\right) \sinh\left(-\frac{\gamma^{(cr)}\sigma^{(cr)}}{kT}\right) \qquad (14)$$

We will ignore temperature effects in this work. Therefore, Equation (14) can be rearranged to a simple one $\dot{\varepsilon}_p^{(cr)} = \beta_0 \sinh\left(\alpha_0 \sigma^{(cr)}\right)$ with and as material constants. Using this equation we obtained much better fitting (see *Fig. 10*) as it is depicted in Figure 9. This results show restrictions and ability of OPR approach in modeling of different types of loading-unloading processes.

CONCLUSION

The unconventional loading-unloading behavior of semi-crystalline polymers as PE and PP is discussed. These observations can be simulated in framework of different phenomenological approaches. However, the correctness of these simulations cannot always be proved, especially in a wide range of strain rates. A novel model (Oshmyan *et al*., 2004, 2005, 2006) allowing strain-induced structural transformations is considered. Supposing loss of the crystalline connectivity at the initial stage of deformation, this model provides satisfactory fitting of experimental data in a small-strain limit. This provides a rough understanding of peculiarities of structure sensitive mechanical response of semi-crystalline polymers. Nevertheless, 2D and 3D simulations should be developed in order to account for relevant parameters characterizing stress-induced structural transformations in semi-crystalline polymers. At the same time it is extremely important to perform comprehensive microscopic investigations to obtain clear understanding of structural objects responsible for mechanical properties and to improve the approach proposed.

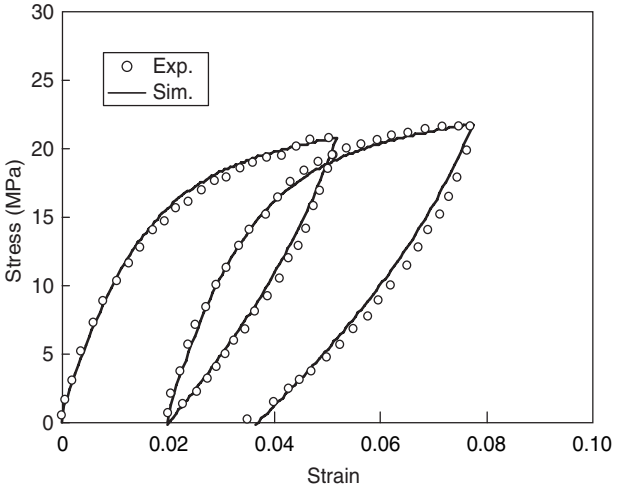

Figure 10

Comparison loading and unloading (two cycles) developed by OPR modified for HDPE.

REFERENCES

Ahzi, S., Makradi, A., Gregory, R.V. and Edie, D.D. (2003) Modelling of deformation and strain-induced crystallization in poly(ethylene terephtalate) above the glass transition temperature. *Mech. Mater.*, **35,** 1139-1148.

André, S., Meshaka, Y. and Cunat, C. (2003) Rheological constitutive equation of solids. *Rheol. Acta*, **42,** 500-515.

Chaboche, J.L. (1997) Thermodynamic formulation of constitutive equations and application to the viscoplasticity and viscoelasticity of metals and polymers. *Int. J. Solids Struct.*, **34**, 2239-2254.

Chambaudet, S., Lesne, P.M. and G'Sell, C. (1998) Simulation of compression tests on polymers and unidirectional composites. *Ann. Composites*, **1**, 3-17.

Colak, O.U. (2004) Modelling deformation behaviour of polymers with viscoplasticity theory based on overstress. *Int. J. Plasticity*, **21**, 145-160.

Drozdov, A.D. and Christiansen, J.C. (2003a) The effect of annealing on the elastoplastic response of isotactic polypropylene. *Eur. Polym. J.*, **39,** 21-31.

Drozdov, A.D. and Christiansen, J.C. (2003b) Modelling the viscoplastic response of polyethylene in uniaxial loading-unloading tests. *Mech. Res. Commun.,* **30**, 431-442.

Ho, K. and Krempl, E. (2000) Extension of the viscoplasticity theory based on overstress (VBO) to capture non-standard rate dependence in solids. *Int. J. Plasticity*, **18**, 851-871.

Hobeika, S., Men, Y. and Strobl, G. (2000) Temperature and strain rate independence of critical strains in polyethylene and poly (ethylene-co-vinyl acetate). *Macromolecules* **33,** 1827-1833.

Kichenin, J., Dang-Van, K. and Boytard, K. (1996) Finite-element simulation of a new two-dissipative mechanisms model for bulk medium-density polyethylene. *J. Mater. Sci.,* **31**, 1653-1661.

Krempl, E. and Ho, K. (2000) An overstress model for solid polymer deformation behaviour applied to Nylon 66. *ASTM Special Technical Publication*, **1357**, 118-137.

Krempl, E. and Khan, F. (2003) Rate (time)-dependent deformation behavior: an overview of some properties of metals and solid polymers. *Int. J. Plasticity*, **19**, 1069-1095.

Oshmyan, V.G., Patlazhan, S.A. and Rémond, Y. (2004) Simulation of small-strain deformations of semi-crystalline polymer: Coupling of structural transformations with stress-strain response. *J. Mater. Sci.,* **39**, 3577-3586.

Oshmyan, V.G., Patlazhan, V. and Rémond, Y. (2005) The Effect of Structural Changes and Nonlinear Character of Plastic Flow on Low Strains in Semi-crystalline Polymers, *Polym. Sci.,* **47,** 346.

Oshmyan, V.G., Patlazhan, S. and Rémond, Y. (2006) Principles of structural mechanical modeling of polymers and composites. *Polym. Sci. Ser. A*, **48,** 1691-1902.

Popelar, C.F., Popelar, C.H. and Kenner, V.H. (1990) Viscoelastic material characterization and modeling for polyethylene. *Polym. Eng. Sci.,* **30,** 577-586.

Rémond, Y. (2005) Constitutive modeling of viscoelastic unloading of short glass fibre-reinforced polyethylene. *Compos. Sci. Technol.,* **65**, 421-428.

Sirotkin, R.O. and Brooks, N.W. (2001) The effects of morphology on the yield behaviour of polyethylene copolymers. *Polymer* **42**, 3791-3797.

Stehly, M. and Rémond, Y. (2002) On numerical simulation of cyclic viscoplastic laws with the large time increment method. *Mech. Time Dependent Mater.*, **6**, 147-170.

Yao, D. and Krempl, E. (1985) Viscoplasticity theory based on overstress. The prediction of monotonic and cyclic proportional and non proportional loading paths of an Aluminium alloy. *Int. J. Plasticity*, **1**, 259-274.

Final manuscript received in October 2006